

## **SATELLITE-BASED DETERMINATION AND ANALYSIS OF GROUNDWATER DROUGHT INDEX TIME SERIES IN EUROPE**

Monika BIRYLO<sup>1</sup>

Faculty of Geoenvironmental Engineering, University of Warmia and Mazury in Olsztyn, Olsztyn, Poland

### **Abstract**

According to the European Drought Observatory, more than 30% of Europe has been under drought warning conditions since 2018. This situation is primarily attributed to a persistent decline in groundwater resources. Satellite observations confirm that groundwater levels have not been recovering; in some regions, they continue to decrease. Data from the Global Gravity-based Groundwater Product (G3P) project, which employs satellite gravimetric measurements, enable continuous monitoring of groundwater variations and provide a globally consistent map of gravity field changes, directly converted into terrestrial water storage variations, of which groundwater is a key component.

This study aims to estimate groundwater storage using models from the Global Gravity-based Groundwater Product derived from the Gravity Recovery and Climate Experiment (GRACE) mission. Based on the estimated groundwater storage, the Groundwater Drought Index (GDI) was calculated for climatically homogeneous regions in Europe, as defined by the Köppen–Geiger climate classification. To enhance the analysis of temporal GDI variations, the index time series was decomposed using the Fourier transform, allowing for the identification of dominant periodic components and long-term trends.

Time series decomposition revealed a strong seasonal dependence of groundwater. The highest levels are observed in spring and the lowest in autumn. A positive trend of groundwater resources was found for Scandinavia region (0.0006 cm). In other areas, a decline in groundwater resources is noticeable since 2016, with the biggest decline in areas of Central and Eastern Europe (-0.0011 cm) and Balkan Peninsula (0.0006 cm).

**Keywords:** groundwater, drought, Europe, climate, Fourier transform, GRACE, G3P, time series decomposition

## **1. INTRODUCTION**

Hydrological drought, agricultural drought, and shortages of groundwater resources are being announced in an increasing number of European countries. Water shortages have serious consequences for people and nature. This is closely related to the loss of groundwater due to rapid climate change, characterised by increasingly higher temperatures and decreasing rainfall. Therefore, considering these

---

<sup>1</sup> Corresponding author: Faculty of Geoenvironmental Engineering, University of Warmia and Mazury in Olsztyn, Olsztyn, Poland  
e-mail: monika.sienkiewicz@uwm.edu.pl

changes, it becomes extremely important to monitor and evaluate changes in drinking water resources constantly. One of the assessment methods is to determine the GDI coefficient (Groundwater Drought Index). Due to numerous satellite missions (climatic, meteorological, and gravitational), obtaining and analysing data over large areas is becoming easier, less labour-intensive, and less time-consuming, and the costs are decreasing. However, to conduct an in-depth analysis of this coefficient, it was decided to decompose the time series of the obtained results.

Since Europe is characterised by a very even climate, according to the Köppen-Geier classification, it is possible to distinguish 6 quite different zones. It is also an area with a very large anthropogenic influence and significant climate changes over the last decades. Combining the study of groundwater from satellite missions, the decomposition of the series using the Fourier transform, and the determination of the GDI are not innovative issues but combining them in one study seems new and very necessary. Moreover, the study of groundwater and its in-depth analysis in such a fragmented area have not interested scientists so far; groundwater is usually studied in areas with vast shortages.

The paper aimed to determine and assess groundwater storage changes and the resulting groundwater storage deviation index changes. The work attempts to support the thesis that groundwater behaves very differently depending on the climate zone, and its deficiency is not so noticeable in every area. In addition, an attempt was made to show the GDI index as a very useful tool for monitoring and assessing droughts and drinking water shortages.

## 2. MATERIALS AND METHODS

### 2.1. Research area

The study carried out research in Europe, divided into identical climatic areas, following the Köppen-Geier division (Fig.1). This division divides the areas in terms of climate types (Table 1), the following were distinguished for study: Area 1: covers the Iberian Peninsula; Area 2: covers islands of Great Britain; Area 3: covers West and South Europe; Area 4: covers Scandinavian Peninsula; Area 5: covers Central and East Europe; Area 6: covers coast of the Aegean Sea. The colours in Fig.1 indicate the climate types according to the classification.

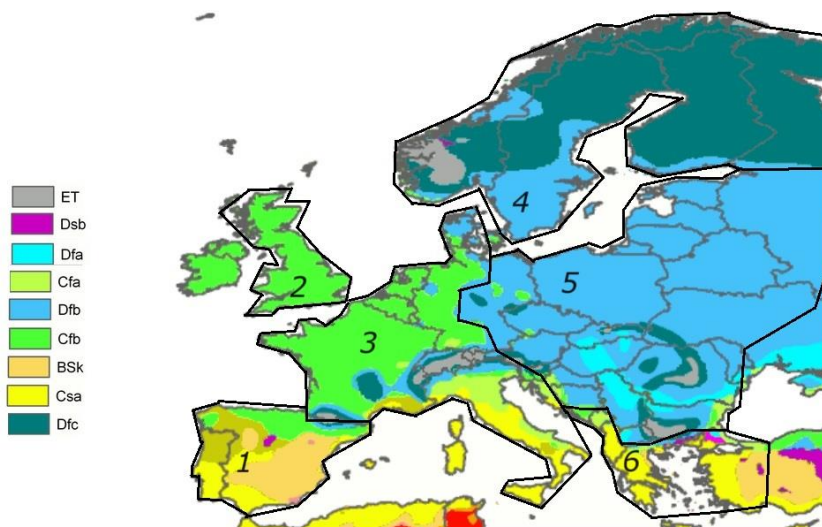


Fig.1. Europe division according to Köppen-Geier climate classification and division into research regions 1, 2, 3, 4, 5, and 6 – case study of the research

Table 1. Designation of the type of climate according to the letters in the Köppen-Geier classification

The first two letters - code	Description	Third letter - code	Description
Bs	steppe climate	k	cold
Cf	humid, moderate climate without dry seasons	a	hot summer
Cf		b	warm summer
Cs	Mediterranean climate: humid, moderate climate with dry summer	a	hot summer
Df	cold, continental climate without a dry season	a	hot summer
Df		b	warm summer
Df		c	cold summer
Dsb	continental with dry summer	b	warm summer
ET	tundra climate	–	–

## 2.2. Used data

The basis for determining the Index is to determine groundwater resources changes, the time series of which were then processed. To complete the task, observations were collected from two satellite missions: GRACE (Gravity Recovery and Climate Experiment) and G3P Copernicus Service (Global Gravity-based Groundwater Product).

The GRACE mission and its continuation, GRACE FO, began in 2002. Its task is to track the Earth's gravity field changes, giving a monthly global product of gravity and, therefore, TWS changes. The most important objective of the GRACE mission was to determine the Earth's gravity field variability with unprecedented and incomparable accuracy. An additional achievement of the mission is numerous climatic observations, closely related to changes in the gravity field. These include changes in the hydrological cycle, the loss of ice mass in large glacier systems, and, consequently, sea level rise. Additionally, the GRACE mission allowed for monitoring ocean circulation processes [Flechtner et al., 2016].

G3P Project (Global Gravity-based Groundwater Product ) aims at combining economy and science to observe groundwater components using remote sensing as part of the announcement by the GCOS (the Global Climate Observing System). The published data are global, monthly distributed, and available since 2002. One of the most important issues covered by the website is the provision of services related to land monitoring products, such as snow water equivalent, soil water index, and water level in rivers. Moreover, the service provides observations regarding climate change products, such as soil surface moisture, glacier mass changes, and water levels in lakes. An additional aspect is a service supporting crisis management by observing river outflow and simulating the behaviour of water storage reservoirs [<http://www.un-igrac.org/special-project/g3p>].

## 2.3. Methods

For groundwater storage (GWS) computation, two sorts of data were acquired: total water storage (TWS) from the GRACE satellite mission and soil moisture (SM) [Dorigo et al., 2017; Pasik, et al., 2023], snow water equivalence (SWE) [Luoju et al., 2021], surface water storage (SWS) [Prudhomme et al, 2024] and canopy (CA).

Total water storage reflects fluctuations in the hydrological cycle and includes various components, such as surface water, snow water, biomass water, soil water, groundwater, and atmospheric

water. As the water cycle is a key phenomenon on Earth, total water storage is strongly influenced by several factors, most notably climate change, and therefore floods and droughts.

Using the TWS GRACE and data from G3P Project, the groundwater storage can be extracted from the TWS, previously described in [Rzepecka et al., 2024; Neves et al., 2020]. As the canopy component has negligible value, for the research presented was omitted. Then, GWS was computed considering the formula [Rzepecka et al., 2016]:

$$GWS = TWS - (SM + SWE + SWS + CA) [cm] \quad (2.1)$$

Having values of GWS, groundwater storage deviation (GWSD) can be estimated. GWSD is the change in the total volume of water stored underground over a specific period, calculated as the difference between groundwater recharge and discharge. A way of assessing groundwater, especially considering drought characteristics, is estimating the groundwater drought index (GDI) based on GWSD calculations. The index can be computed by normalizing the groundwater storage deviation [Thomas et al., 2017]:

$$GDI = \frac{(GWSD - \overline{GWSD})}{st.dev.(GWSD)} [cm] \quad (2.2)$$

Where:  $GWDI$  – groundwater drought index,  $\overline{GWSD}$  – mean groundwater storage deviation,  $std(GWSD)$  - standard deviation of groundwater storage deviation.

For further analysis, time series are decomposed into the following components: trend, seasonality, and random fluctuation to find seasonal patterns (annual and semi-annual), and random fluctuations (noise), which are the original signal minus trend and a seasonal component. Thus, by using all three components, you can reconstruct the original time series values. In the research, an additive model of decomposition was used, which constitutes the following formula:

$$Time\ series = Trend + Seasonality + Noise \quad (2.3)$$

For mathematical signal analysis, the obtained GDI time series (input signal) were then decomposed into sinusoids in the form of the Discrete Fourier Transform (DFT). The Discrete Fourier Transform is a transform that aims to analyse a finite signal. This analysis can be described as a computationally efficient representation of the frequency of signals over time. These signals are obtained from the coefficients of the Fourier series.

The output signal is frequency of the time series. This process is constituting decomposition, the opposite is synthesis. The output is composed of the two parts: real ( $Re$ ) and Imaginary ( $Im$ ), which in fact are amplitudes of sine and cosine waves. The sine and cosine waves satisfy the equations  $c_k[i] = \cos\left(\frac{2\pi k i}{N}\right)$ , and  $s_k[i] = \sin\left(\frac{2\pi k i}{N}\right)$ , where  $N$  denotes the number of signal samples in one period or the length of the analyzed data sequence, and  $k$  denotes the frequency index, the number of the harmonic for which the DFT coefficient is calculated.. Using a polar notation of synthesis, it can be written:

$$A \cos(x) + B \sin(x) = M \cos(x + \theta) \quad (2.4)$$

Where:  $M$  is a magnitude and  $\theta$  is a phase, both computed from  $Re$  and  $Im$  and:

$$M(X)[k] = \sum_{k=0}^{N/2} \sqrt{(ReX[k]^2 + ImX[k]^2)} \text{ and } \theta(X)[k] = \text{atan}\left(\frac{ImX[k]}{ReX[k]}\right) \quad (2.5)$$

### 3. RESULTS

The research began with the determination of the groundwater storage changes, according to formula (2.1). Each tested element ( $\Delta TWS$ ,  $\Delta SM$ ,  $\Delta SWS$ ,  $\Delta SWE$ ) is characterised by strong and easily noticeable seasonal variability, with upper and lower peaks in similar periods across the continent (Fig.2, Fig.3, Fig.4, Fig.5).

When analysing the  $\Delta TWS$  time series (Fig.2), it is easy to notice that each area selected for research records the highest values in the spring months and the lowest in the autumn periods. However, the studied areas differ significantly in terms of the amplitudes of TWS changes. In the years 2002÷2006, all areas had quite similar lowest  $\Delta TWS$  values (-5 cm) but differed in terms of the highest values. However, areas 3 and 6 have a maximum value of about 13 cm, and the remaining areas are about 5 cm. In the years 2007÷2009, the highest values overlap at approximately 7 cm, except for the maximum values of area 2 (maximum values about 2 cm). Changes occur when it comes to minimum values. Area 6 stands out here, achieving very low TWS changes at -11 cm. In area 2, TWS changes are small, approximately -1 cm, and the remaining examined areas reach -3 cm. From 2010 until the end of the GRACE mission, the level for area 2 remains stable, with small peaks, like those in previous years. The remaining areas, apart from area 5, are characterised by apparent amplitudes (between -7 and 5 cm). Area 5 reaches maximum values like areas 1, 3, 4, and 6, but minimum values reach -10 cm, and in 2010, 2014, and 2015, even -15 cm. The GRACE-FO mission began in 2018. During this period, the  $\Delta TWS$  values for areas 5 and 6 reach lower values every year until the end of the study period (from -13 cm in 2018 to -20 cm in 2022). For these two areas, the minimum values are positive only in 2018, and in the following years, they do not exceed 0 cm. The values of changes in area 1 also decrease during the GRACE-FO mission, reaching negative values in the range of max. 0 cm and min. -13 cm. Area 4 stands out, with values much higher than other areas, reaching maximums at a constant, non-decreasing level of 5 cm, and in 2020, even 12 cm. The values for area 2 do not differ from previous years.

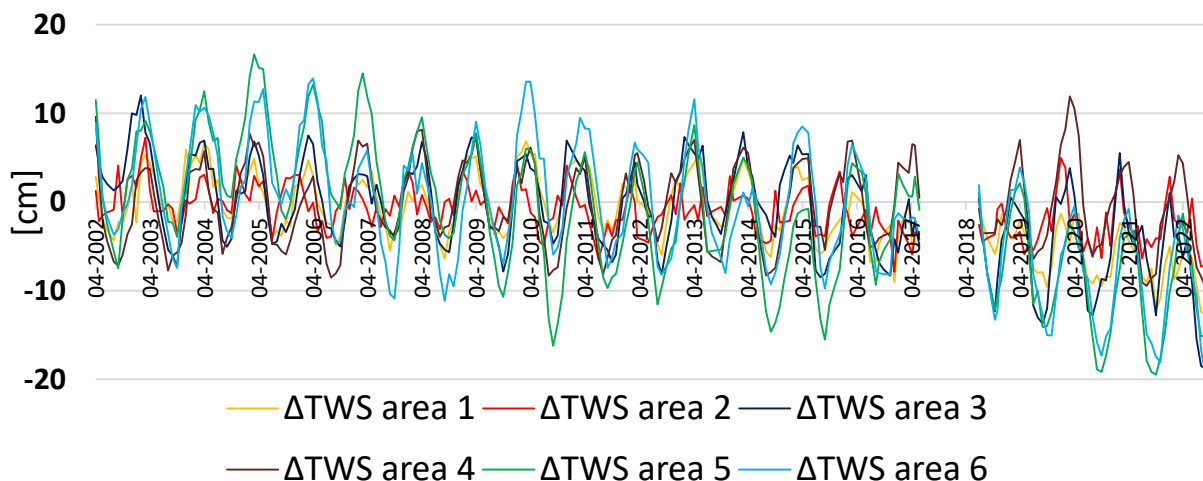


Fig.2. Total water storage change for areas 1, 2, 3, 4, 5, 6

Soil moisture was determined to a depth of 2 m (Fig.3). Significant differences are noticeable. The upper and lower peaks appear in similar periods (achieving maximum in spring at about 6 cm, and minimum in autumn at about -7 cm) for areas 1, 3, 5, and 6, and are slightly equal in amplitude of changes. In the period 2008 - 2011, the time series of area 1 stands out, reaching a 2 cm higher level in the maximum periods compared to the remaining ones, and the time series of area 6 reaches a 1 cm lower level in the

minimum periods. All four areas have a regular, sinusoidal waveform with alternating maximum and minimum values. As for area No. 2, it reaches maximum and minimum soil moisture values in the same periods as the previously mentioned areas. However, the amplitudes of the changes are much smaller, ranging on average from  $-2 \div 2$  cm. At the end of the analysed period, from 2016, the maximum values coincide with the other areas already discussed, but this is related to a decrease in the remaining values. The highest and lowest values for area 4 are in antiphase to the other five areas. At the beginning of the examined period, until 2007, the minimum and maximum values are only positive (from 0 to 4 cm). Then, until 2013, the values are in the range of  $-2 \div 2$  cm, and by the end of the period under study, they reach the range of  $-6 \div 2$  cm.

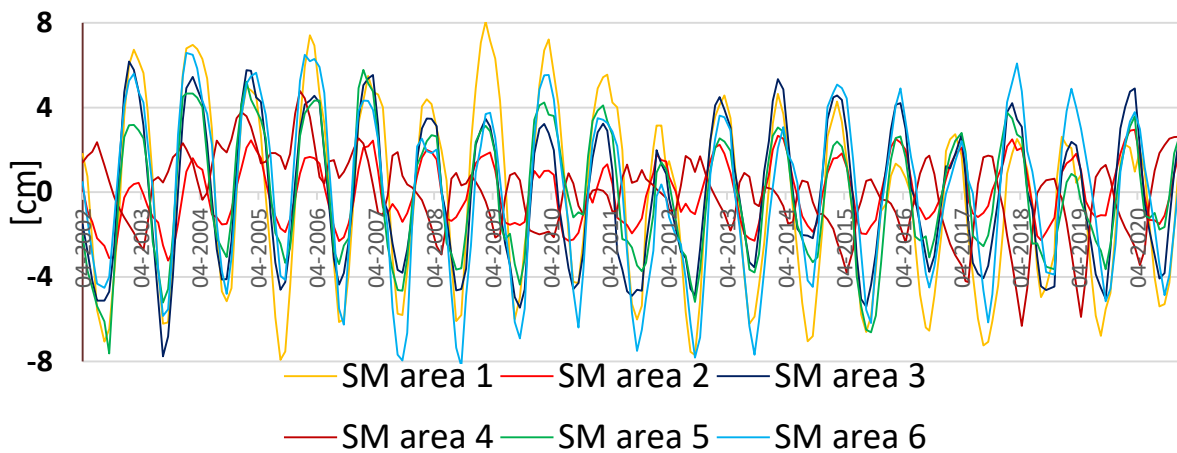


Fig.3. Soil moisture changes for areas 1, 2, 3, 4, 5, and 6

Snow water equivalence (Fig.4) is characterised by very strong seasonality and location dependence. The phenomenon is noticeable in the winter months, and the values are higher further north and east. The highest SWE values and the largest amplitudes were observed in area 4 ( $-3 \div 9$  cm), zero values throughout the studied period were recorded for areas 1 and 2.

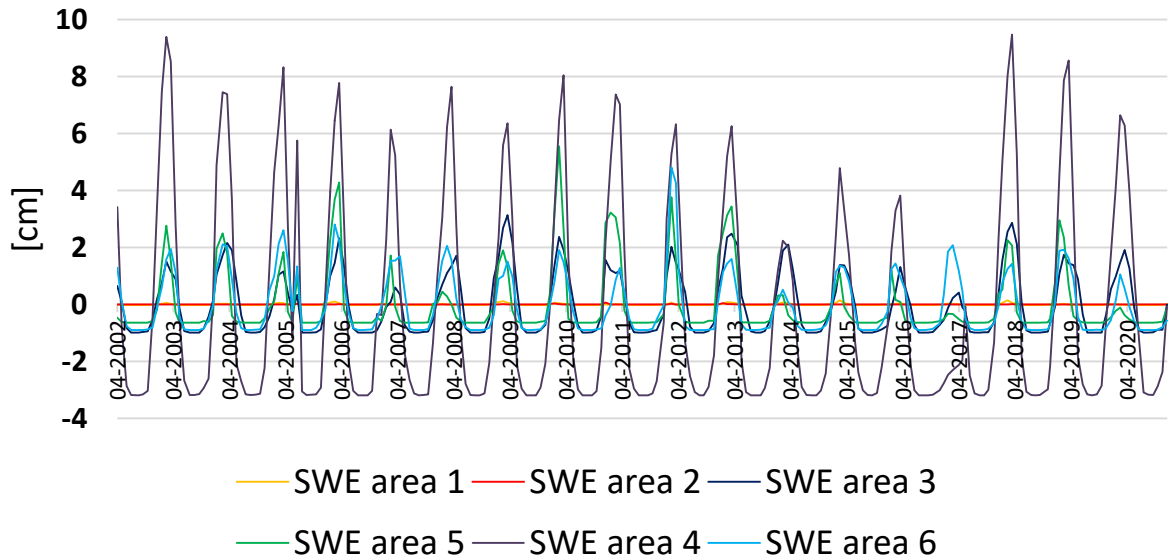


Fig.4. Snow water equivalence change for areas 1, 2, 3, 4, 5 and 6

The SWS (Fig.5) is strongly dependent on water reservoirs, which occur largely in post-glacial areas (e.g. Scandinavia). This is noticeable in the presented time series, in which area 4 stands out with high values and large amplitudes (-2÷2 cm). The phenomenon of seasonality is also strong (the highest values in spring and the lowest in winter); the same phenomenon is noticeable for areas 3, 4, and 6. Areas 1 and 2 are characterised by small fluctuations in SWS changes (values close to 0 throughout the year) and without a clear impact on seasons.

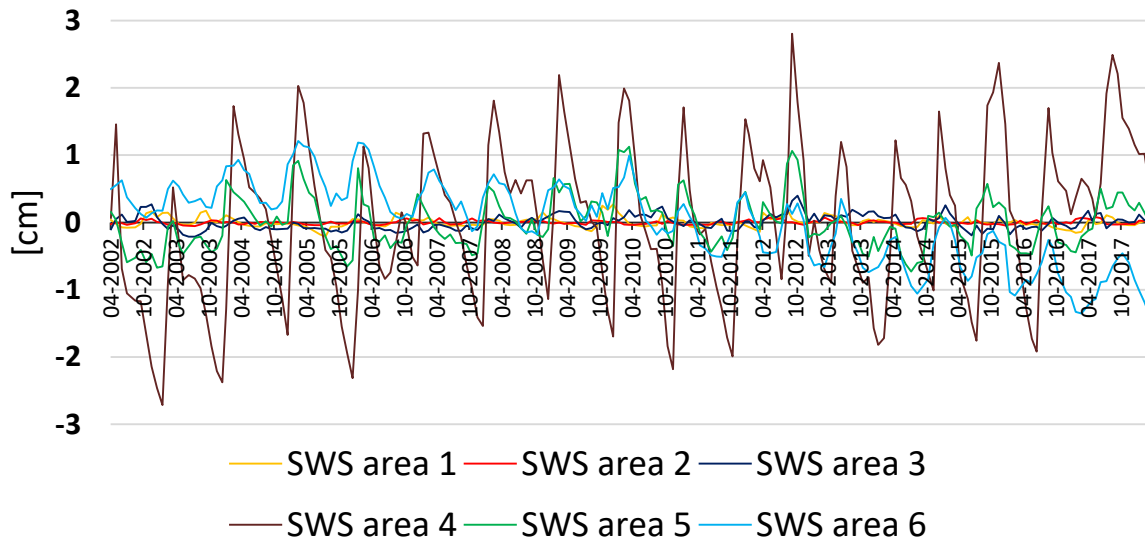


Fig.5. Surface water storage for areas 1, 2, 3, 4, 5, 6

In the next step, groundwater resources changes were determined following formula (2.1), which were then converted into GWS anomalies (GWSA) (Appendix 1). The first period of research, from the GRACE mission, shows groundwater changes in a synchronous seasonality, with the highest values in

the spring/summer period and the lowest in the autumn/winter period, with 2/3 3-month delay between areas. GWSA studies during the operation of the GRACE-FO mission have shown that almost all areas (except area 4) reach very low values - the maximum values slightly exceed 0 cm for area 2. Basic statistical characteristics (maximum, minimum, mean, and standard deviation) for each region and every element of groundwater storage are presented in Table 2.

Table 2. Basic statistical characteristics of TWS, soil moisture, snow water equivalent, and surface water storage

		Max.	Min.	Mean	St. Dev.
TWS	Area1	6.855	-12.666	-1.382	4.107
	Area 2	7.251	-7.868	-1.115	2.661
	Area 3	12.038	-18.860	-0.911	5.408
	Area4	11.912	-9.748	-0.260	4,675
	Area 5	16,660	-19,461	-1,655	7,749
	Area 6	13,949	-19,947	-1,042	7,157
Soil moisture	Area1	8.058	-7.922	-0.267	4.215
	Area 2	2.956	-3.229	-0.010	1.459
	Area 3	6.174	-7.746	-0.124	3.322
	Area4	4.778	-6.313	-0.065	1.834
	Area 5	5.775	-7.619	-0.135	2.897
	Area 6	6.577	-8.222	-0.120	3.845
Snow Water Equivalent	Area1	0.146	-0.018	0.000	0.030
	Area 2	0.065	-0.003	0.000	0.007
	Area 3	3.143	-0.991	-0.011	1.084
	Area4	9.474	-3.190	-0.074	3.676
	Area 5	5.551	-0.638	-0.012	1.146
	Area 6	4.812	-0.891	-0.046	1.074
Surface Water Storage	Area1	0.271	-0.213	0.000	0.075
	Area 2	0.077	-0.056	0.000	0.029
	Area 3	0.395	-0.211	0.000	0.108
	Area4	2.805	-2.711	0.000	1.159
	Area 5	1.123	-0.729	0.000	0.386
	Area 6	1.213	-1.403	0.000	0.599

Then, following formula (2.2). the GDI index was determined (Fig.6). The GDI time series has a pronounced cyclical character. Most of the amplitudes of changes range between -2 and +2 cm, with higher values temporarily occurring in area 2 or area 4. Several periods of greater instability were observed, particularly in 2004–2005, 2010–2012, and 2016–2018. After 2018, the data appears more stable, with smaller deviations. Area 5 and area 6 are often in antiphase with the other areas being examined.

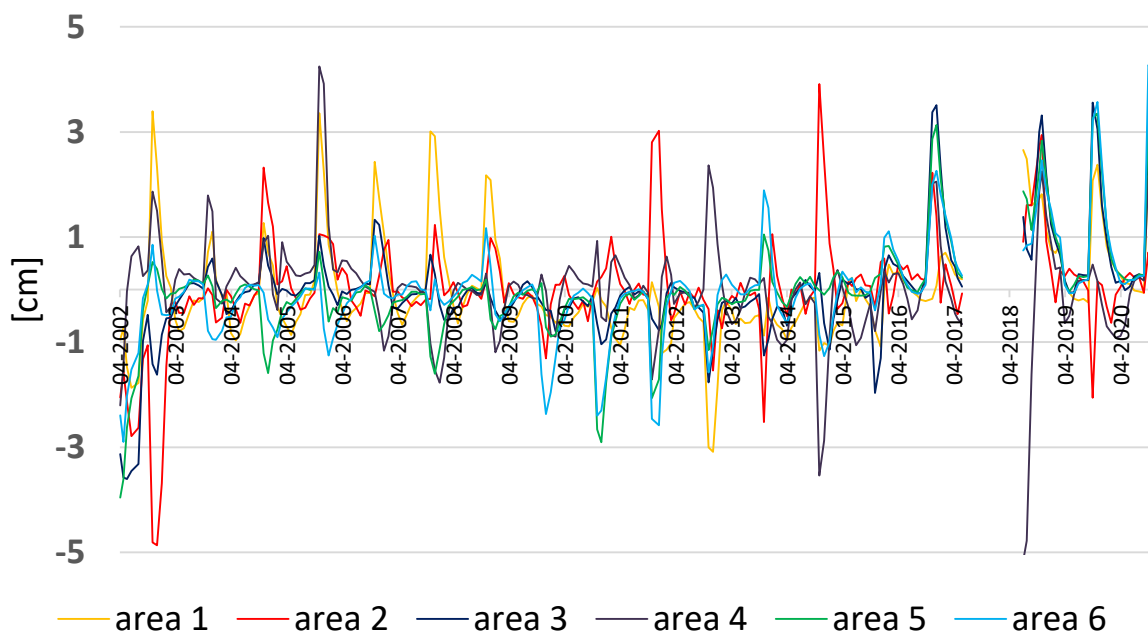
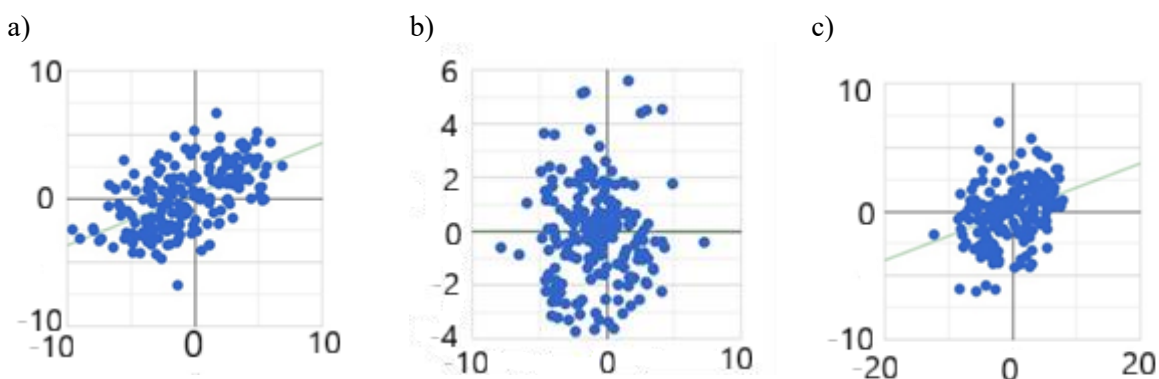


Fig.6. Groundwater Drought Index for areas 1, 2, 3, 4, 5, 6

The Mann-Kendall test is used to detect and test the significance of trend changes in time series, which is used to determine whether there is a monotonic trend in the data (upward or downward). The Mann-Kendall test analyses the sign of the difference between successively measured values [Liu et al, 2022; Zhang et al., 2016].

The smallest difference between consecutive trend values was observed in area 3 (Fig.7c). The most negative trend, as indicated by the Mann-Kendall test, is observed in area 2 (Fig.7b). The rest of the areas are not monotonic (Figures 7b, 7c, 7d, 7e, 7f). The most monotonic and linear trend is noticed for area 1 (Fig.7a). Most negative values of the trend are characteristic of area 4 (Fig.7d).



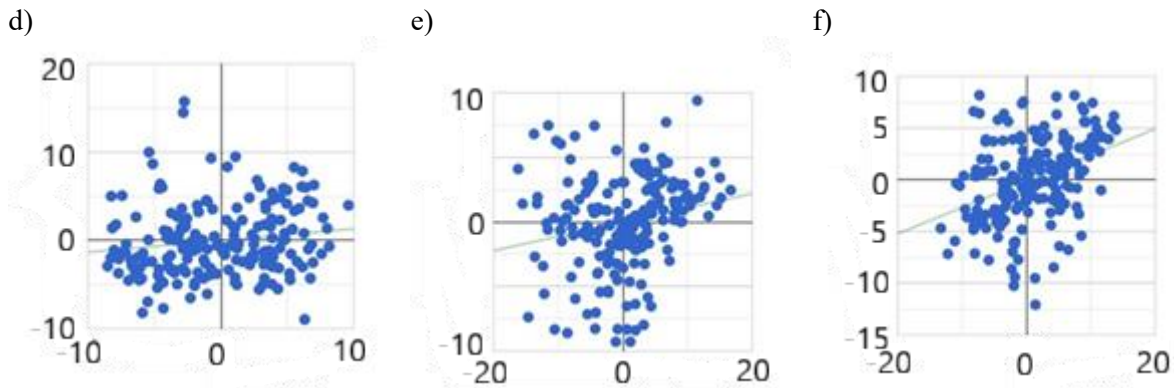


Fig.7. Mann-Kendall test for areas 1 (a), 2 (b), 3 (c), 4 (d), 5 (e), 6 (f)

The following parameters were calculated for each area: annual seasonality, random noise of annual seasonality, semi-annual seasonality, magnitude, phase, and synthesis of magnitude and phase for the signal decomposition. All areas are characterized by well-noticeable annual (Fig.8a, Fig.9a, Fig.10a, Fig.11a, Fig.12a, Fig.13a) and semi-annual seasonality (Fig.8c, Fig.9c, Fig.10c, Fig.11c, Fig.12c, Fig.13c). However, the annual seasonality of area 1 is characterised by smooth transitions between the highest and lowest values (Fig.8a). The most irregular course of the seasonality chart was observed in the case of area 4 (Fig.11a). For other areas, small fluctuations were observed preceding or following the main period of GDI increase in the season. A semi-annual seasonality analysis was also performed, in which smoother and regular series were noticed, especially for areas 1, 2, 4, and 6.

Random noise was also determined for annual seasonality in reference to formula (2.3), transforming it into the form:  $Noise = Time\ Series - Annual\ Seasonality - Trend$ . The random noise lets us detect anomalies and outliers, so unexplained variance and volatility cannot be explained by a periodic signal. It can be noticed that the peaks do not occur in regular intervals. The highest range of random noise values was found for area 4 (particularly negative values, Fig.11b) and area 1 (but are evenly distributed above and below line 0, Fig.8b). Areas 3, 5, and 6 have a similar distribution of the random noise range (-2 to 2 cm, Fig.10b, Fig.12b, and Fig.13b).

Then, the elements of the Fourier transform, i.e. magnitude and phase, were determined, according to formula (2.5). Magnitude informs about the dominance of the annual seasonality. Interesting conclusions were found based on the magnitude analysis. Signal produces impulses in 20, 40, 60, 80, and 100, and usually the values are smaller further. However, by far the highest range was observed for area 1 (reaches as much as 40 Hz, Fig.8d). Areas 2, 3, and 4 have a range of up to 20 Hz (Fig.9d, Fig.10d, and Fig.11d), while areas 5 and 6 have a range of up to 12 Hz (Fig.12d and fig.13d). Interestingly, the amplitude spectra show that the phases of individual spectral components in 20 and 40 are equal for areas 4, 5, and 6. The next step is the determination of the phase, which tells us how quickly the time series increases/decreases. The phase spectrum shows the phase of individual spectral components, informing how all the frequency components align in time (Fig.8e, Fig.10e, Fig.11e, Fig.12e, Fig.13e). The only exception is area 2, followed by a very long period of exclusively positive values (Fig.9e). The range of values for all studied areas is the same (approximately  $-4 \div 3$  Hz).

The last step was signal decomposition using the Fourier transform. The Fourier transform moves a signal from the time domain to the frequency domain and aims to represent the time series in a much simpler form – a form of trigonometric functions. Decomposition aims to identify the contributions of each observation within the overall acquired signal [Das and Barman, 2025]. The effect of the transform

is presented in Fig.8f, Fig.9f, Fig.10f, Fig.11f, Fig.12f, and Fig.13f. Every decomposed signal is regular, seasonal, and much smoother than the raw GDI signal, and comparable to the annual seasonal signal.

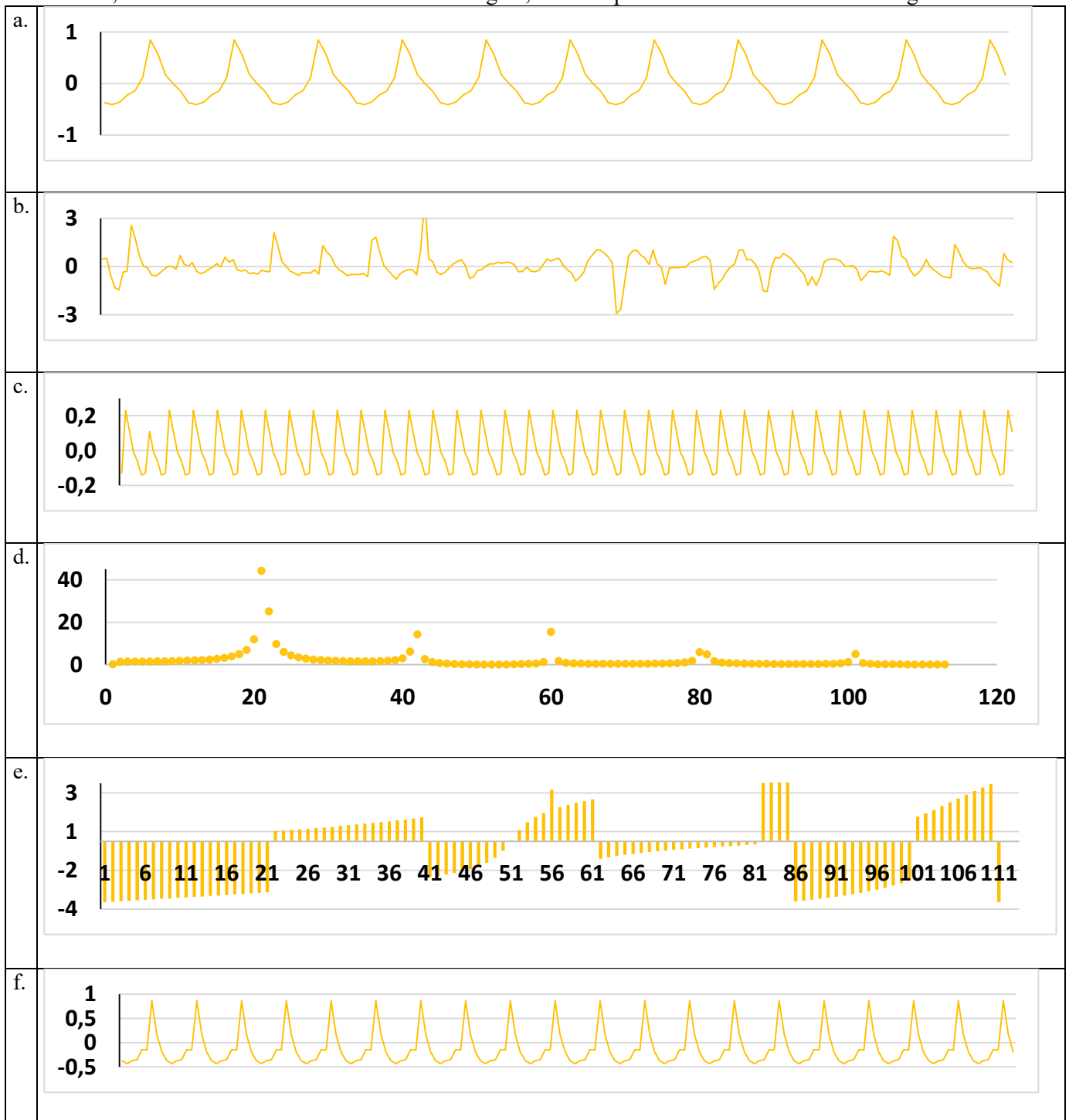


Fig.8. Area 1: a. Annual seasonality; b. Random noise of annual seasonality; c. Semi-annual seasonality; d. Magnitude; e. Phase; f. Synthesis of magnitude and phase

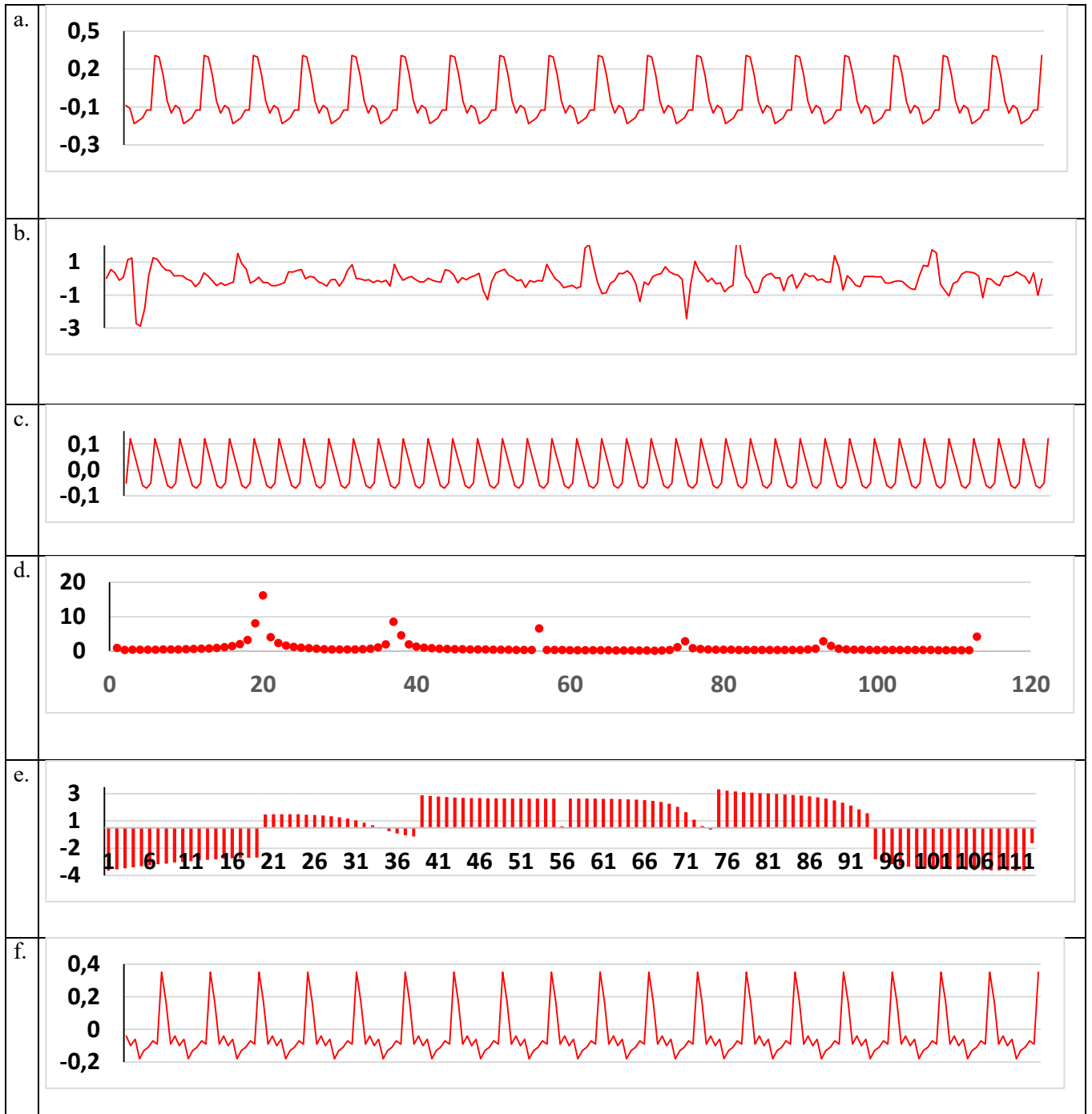


Fig.9. Area 2: a. Annual seasonality; b. Random noise of annual seasonality; c. Semi-annual seasonality; d. Magnitude; e. Phase; f. Synthesis of magnitude and phase

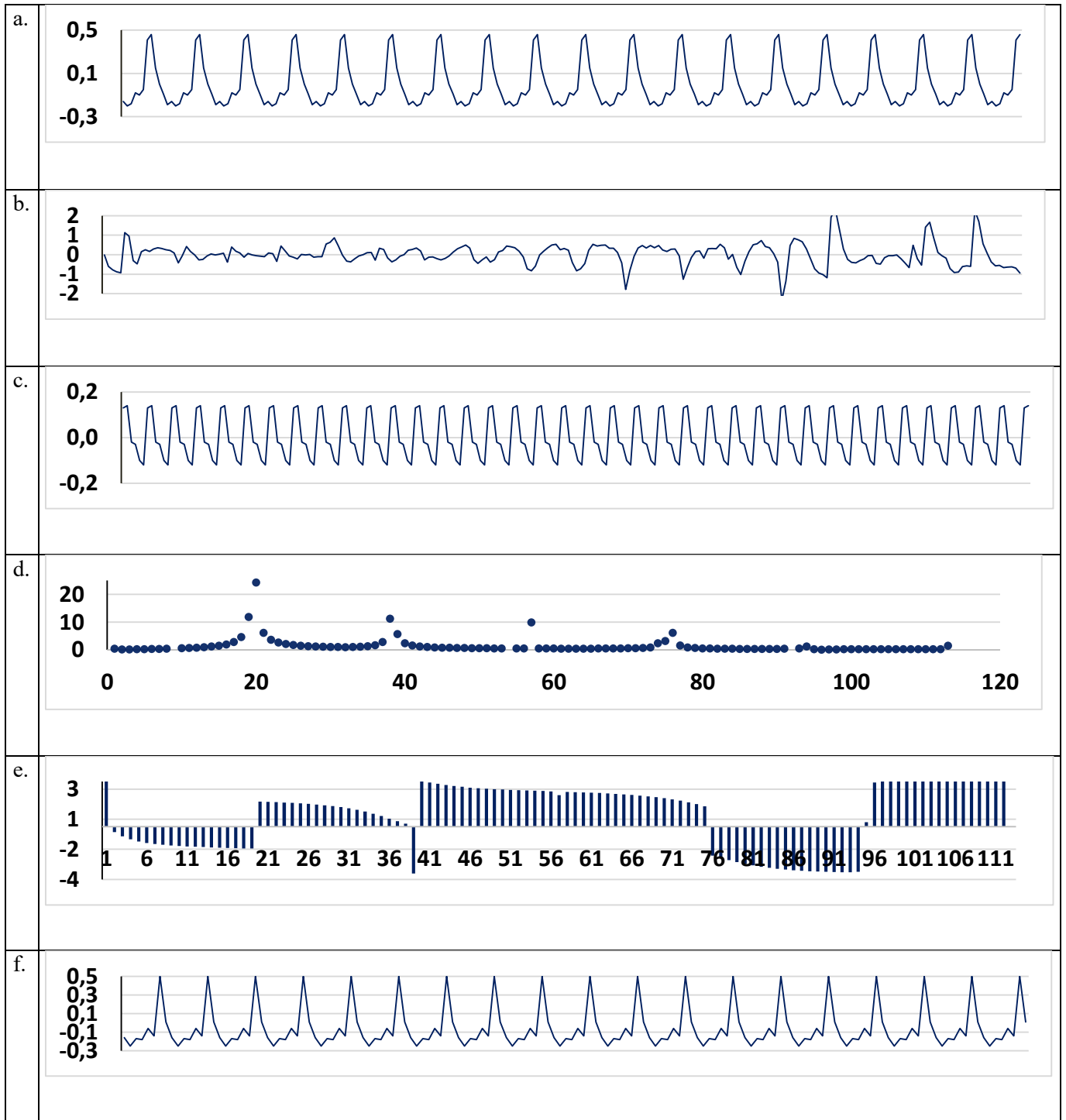


Fig.10. Area 3: a. Annual seasonality; b. Random noise of annual seasonality; c. Semi-annual seasonality; d. Magnitude; e. Phase; f. Synthesis of magnitude and phase

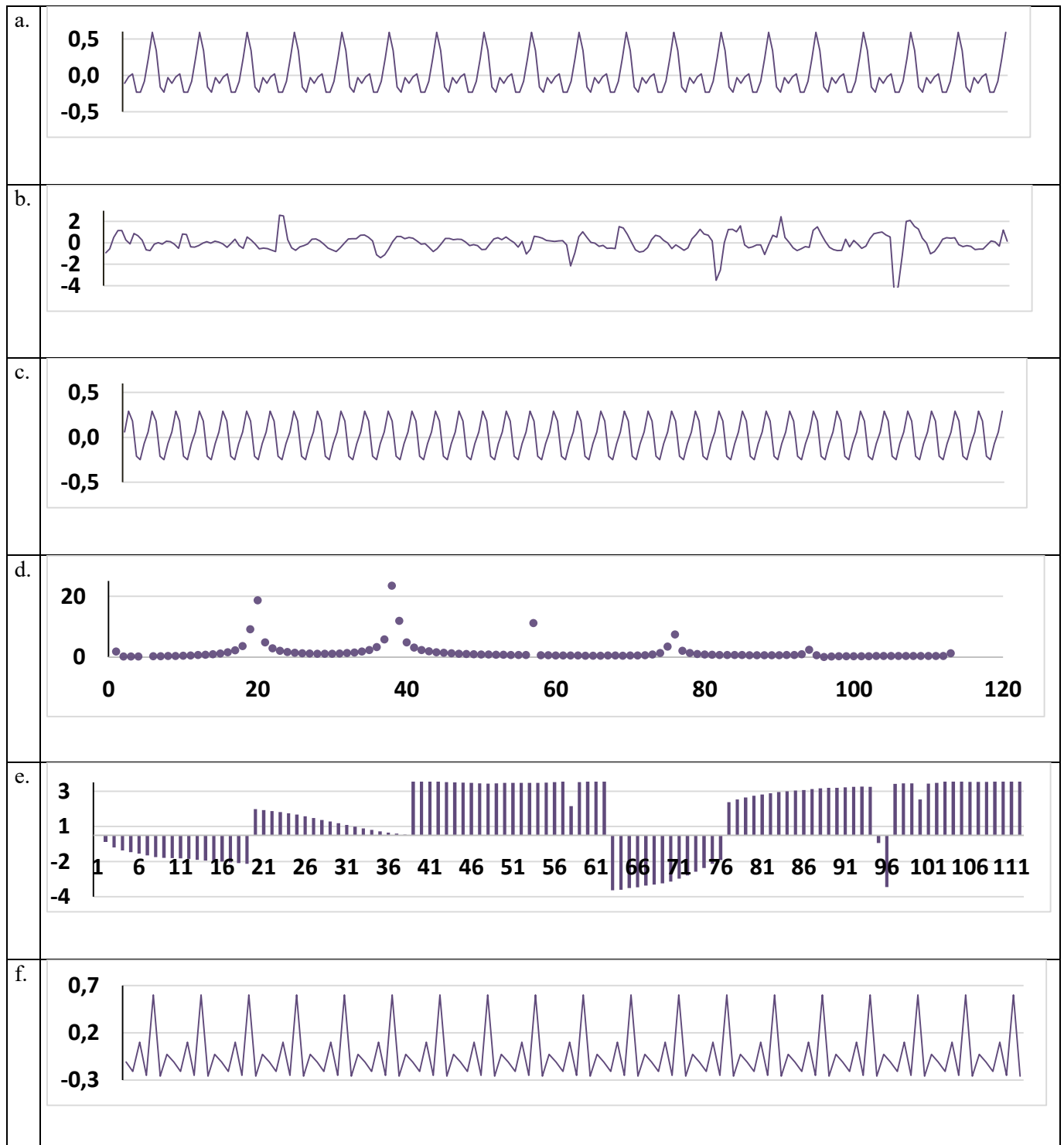


Fig.11. Area 4: a. Annual seasonality; b. Random noise of annual seasonality; c. Semi-annual seasonality; d. Magnitude; e. Phase; f. Synthesis of magnitude and phase

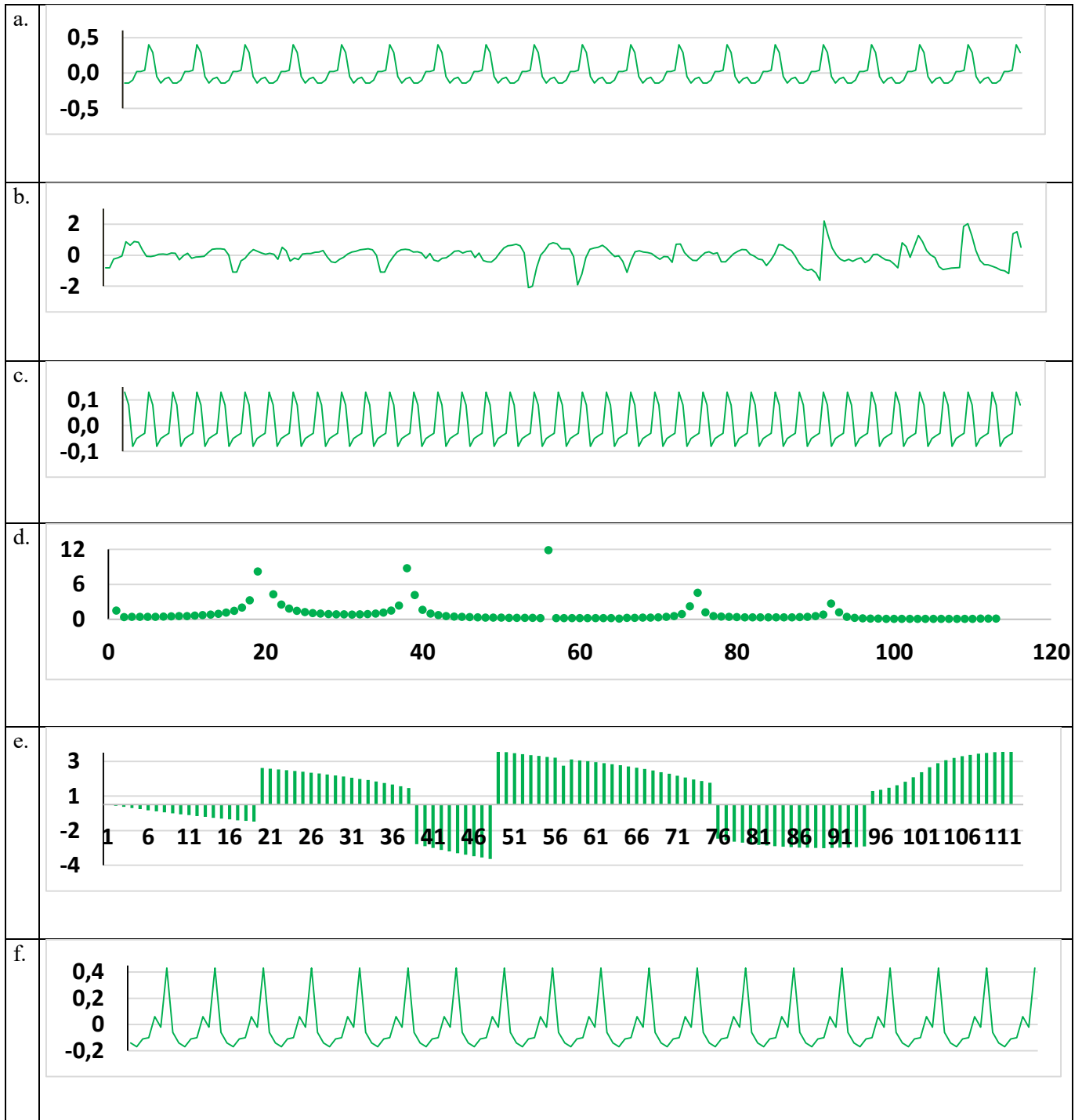


Fig.12. Area 5: a. Annual seasonality; b. Random noise of annual seasonality; c. Semi-annual seasonality; d. Magnitude; e. Phase; f. Synthesis of magnitude and phase

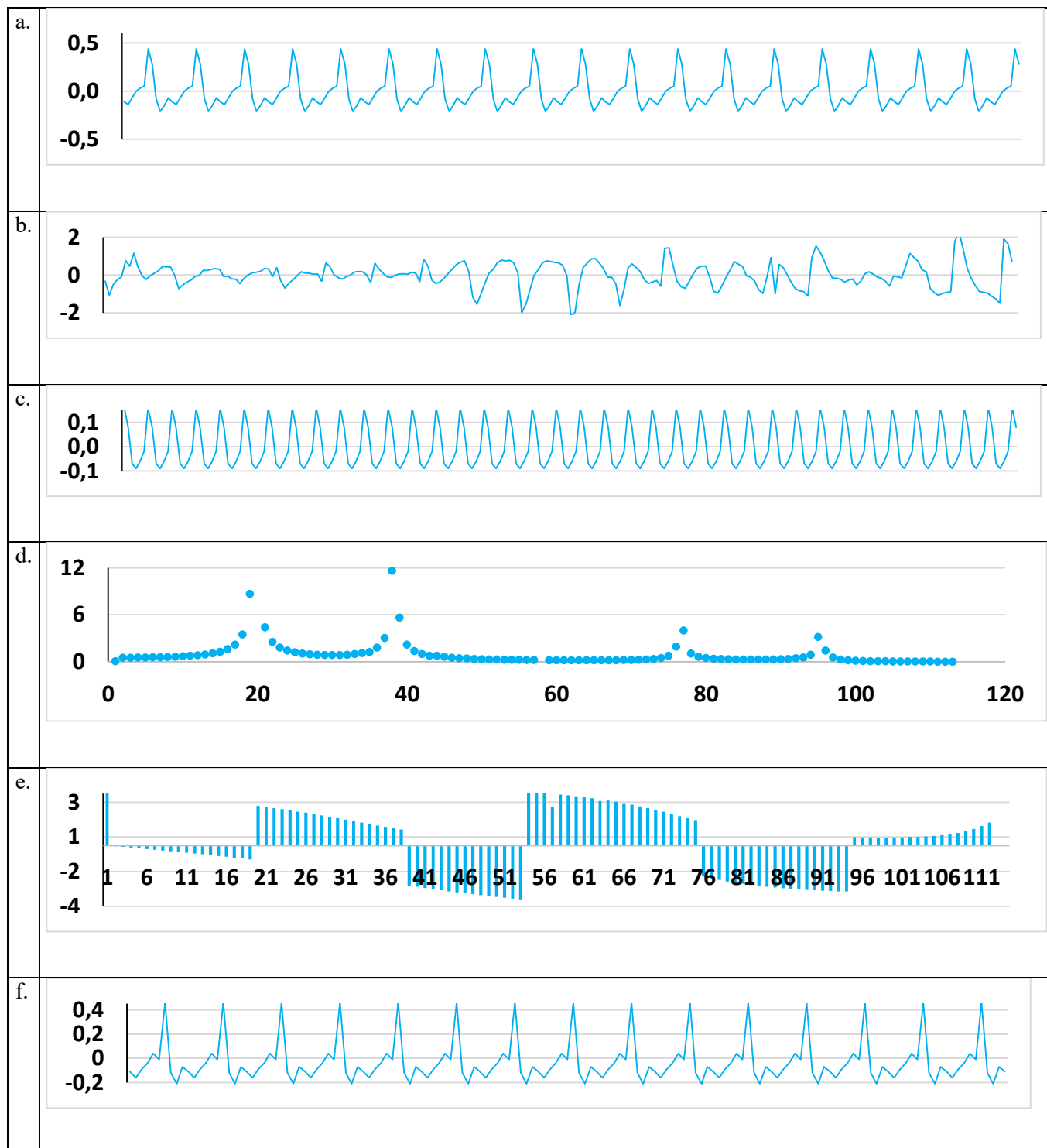


Fig.13. Area 6: a. Annual seasonality; b. Random noise of annual seasonality; c. Semi-annual seasonality; d. Magnitude; e. Phase; f. Synthesis of magnitude and phase

#### 4. DISCUSSION

Signal decomposition is a very widely used numerical tool that can be used in different fields of physics, engineering, and mathematics. Such a wide range of possibilities for using the Fourier series allows it to be used in the research presented in the paper. Its feature is that it allows describing a time series as a frequency rather than as a function of time. Groundwater is an extremely important element of the economy because it is not only a source of drinking water, but also the basis for the functioning of industries, including the processing and food industries. However, the analysis of groundwater changes in large areas is less frequently included in scientific analyses and areas such as: South Asia [Alshehri and Mohamed, 2023; Long et al., 2016], China [Guo et al., 2022, Zhao et al., 2023, Li et al., 2023, Adem et al., 2024], or Africa [Ramjeawon et al., 2022; Mohasseb et al., 2024, Agutu et al., 2019]. As far as Europe is concerned, the topic of groundwater changes and their study using satellite missions and models seems to be of less interest among scientists. It is especially worth noting that groundwater resources in Europe were considered infinite. However, the current situation proves that water is disappearing and is at risk of almost irreversible contamination. This condition was confirmed as part of the European Surface project [<https://www.journalismfund.eu/under-surface-untold-crisis-european-groundwater>, accessed: 5.09.2024]. In Xanke and Liesch [2022], it was noted that in Euro-Mediterranean countries, due to anthropogenic use and climate influence, there has been a significant decrease in groundwater levels and a loss of balance between replenishing water from rainfall and its abstraction. Based on the research, it was found that the average annual trends experienced a significant decrease in GWS (in approximately 70% of the study area) - i.e. a huge loss of acquirers was found (the trend for the selected Euro-Mediterranean region was found: -2.1 mm/year). In comparison. Gebrechorkos et al. [2025] found that 82% of Europe was experiencing drought. with approximately 50% experiencing severe drought. Rakovec et al. [2022] found that 40% of the continent was experiencing drought throughout the year. Ionita and Nagavciuc [2021] found that over 60% of the continent was affected by moderate or severe drought.

In the presented study, a positive trend was found for area 4 (0.0006 cm/2002-2020,  $R^2=0.891$ ). This is an area of Scandinavia that is rich in surface water, has the coldest climate in Europe, and is covered in the north by glaciers that melt and feed underground reservoirs. The enormous influence of glaciers and their melting on the groundwater level in Scandinavia, especially in its northern part, was also described in Rzepecka et al. [2024]. It should also be mentioned that for all areas there has been a noticeable decline in groundwater resources since 2016. All other areas show negative trends, with large declines for areas 5 (-0.0011 cm/2002-2020,  $R^2=0.3112$ ) and 6 (0.0006 cm/2002-2020,  $R^2=0.247$ ) and moderate negative trends for areas 1 (-0.0004 cm/2002-2020,  $R^2=0.094$ ), 2 (-0.0004 cm/2002-2020,  $R^2=0.168$ ), 3 (-0.0007 cm/2002-2020,  $R^2=0.228$ ). The causes of water decline include increased groundwater consumption, global warming, and, as a result, lower rainfall and decreased groundwater replenishment [Aureli et al. 2008; Zhang et al. 2020]. Although Xanke and Liesch [2022] stated that climate seems to be the least significant factor, based on studies conducted in Europe, divided into climate zones, it seems to confirm that in milder climates this loss is smaller. On the other hand, Garcia Silva et al. [2024] stated that stable groundwater levels are recorded in southwestern Europe. The study found that 20% of wells with rising groundwater levels and 68% with stable levels, which means that the problem was identified in about 10% of South Europe's wells. It may seem that the discrepancies shown by Garcia Silva et al. [2024] are caused by differences in the scale of observation. Despite the division into climate zones. areas interact with each other. While research typically focuses on regions at risk of aridity. such as river basins. This study focuses on the entire continent. Additionally, a comprehensive analysis of the estimated GDI signals is presented. providing a comprehensive picture of groundwater threats in Europe.

## 5. CONCLUSIONS

In the paper, groundwater storage changes and the resulting groundwater storage deviation index changes were determined for the climatic zones of Europe for the period 2002-2020. GRACE mission observations and their product, G3P, were taken for calculations. For better perception and analysis, the time series Fourier transform was used for the decomposition. Based on the research, it can be concluded that:

- The results of the presented study confirmed the observations of earlier studies and monitoring programs, which signaled falling groundwater levels, especially in southern Europe. Areas with a temperate climate are characterised by a smaller decline in resources, but the situation here is also alarming. Only in the northern parts of Europe is the trend positive but considering the two-decade period of study. In all regions, there has been a noticeable year-on-year decrease since 2016.
- It was found that trend analyses of GWS data from GRACE provide a very reliable picture of groundwater resources and use
- The seasonality study and series decomposition showed a strong seasonal dependence of groundwater, with the highest levels in spring and the lowest in autumn. This is closely correlated with solar radiation, and thus with evaporation and rain supply. This proves that the greatest influence on GWS is climate and its changes.

## REFERENCES

1. Adem, E et al. 2024. Land subsidence and groundwater storage change assessment using InSAR and GRACE in the arid environment of Saudi Arabia. *Natural Hazards – Springer* **120**(11). <https://doi.org/10.1007/s11069-024-06733-8>.
2. Agutu, NO et al. 2019. GRACE-derived groundwater changes over Greater Horn of Africa: Temporal variability and the potential for irrigated agriculture. *Science of The Total Environment* **693**(25). 133467. <https://doi.org/10.1016/j.scitotenv.2019.07.273>.
3. Alshehri, F and Mohamed, A 2023. Analysis of Groundwater Storage Fluctuations Using GRACE and Remote Sensing Data in Wadi As-Sirhan, Northern Saudi Arabia. *Water* **15**(2), 282; <https://doi.org/10.3390/w15020282>.
4. Aureli, A et al. 2008. Groundwater resources in the Mediterranean region: importance, uses and sharing. <https://www.iemed.org/publication/groundwater-resources-in-the-mediterranean-region-importance-uses-and-sharing/>. Accessed on 7.09.2025.
5. Das, P and Barman, P 2025. An Overview of Time Series Decomposition and Its Applications. *Applied and Theoretical Econometrics and Financial Crises. (pp.1-15) Publisher: IntechOpen Limited*. DOI: 10.5772/intechopen.1009268.
6. Dorigo, W et al. 2017. ESA CCI Soil Moisture for improved Earth system understanding: State-of-the art and future directions. *Remote Sensing of Environment* **203**, p. 185—215. <https://doi.org/10.1016/j.rse.2017.07.001>.
7. Flechtner, F et al. 2016. What Can be Expected from the GRACE-FO Laser Ranging Interferometer for Earth Science Applications? Reprinted from *Surveys in Geophysics Journal* **37**, DOI 10.1007/978-3-319-32449-4\_11.
8. Gebrechorkos, SH et al. 2025. Warming accelerates global drought severity. *Nature*. **642**. <https://doi.org/10.1038/s41586-025-09047-2>.

9. Guo, Y et al. 2022. Evaluation of Groundwater Storage Depletion Using GRACE/GRACE Follow-On Data with Land Surface Models and Its Driving Factors in Haihe River Basin, China. *Sustainability* **14**(3). <https://doi.org/10.3390/su140311>.
10. Ionita, M and Nagavciuc, V 2021. Changes in drought features at the European level over the last 120 years. *NHESS* **21**(5), Pages: 1685–1701. <https://doi.org/10.5194/nhess-21-1685-2021>.
11. Li, W et al. 2024. The analysis on groundwater storage variations from GRACE/GRACE-FO in recent 20 years driven by influencing factors and prediction in Shandong Province, China. *Scientific Reports* **14**, 5819. <https://doi.org/10.1038/s41598-024-55588-3>.
12. Liu, S et al. 2022. Trend Test for Hydrological and Climatic Time Series Considering the Interaction of Trend and Autocorrelations. *Water* **14**, no. 19: 3006. <https://doi.org/10.3390/w14193006>.
13. Long, D et al. 2016. Have GRACE satellites overestimated groundwater depletion in the Northwest India Aquifer? *Scientific Report* **6**, 24398. <https://doi.org/10.1038/srep24398>.
14. Luoju, K et al. 2021. GlobSnow v3.0 Northern Hemisphere snow water equivalent dataset *Sci Data* **8**(163). <https://doi.org/10.1038/s41597-021-00939-2>.
15. Mohasseb, HA et al. 2024. Estimation of groundwater storage variations in African river basins: Response to global climate change using GRACE and GRACE-FO among past two decades. *Advances in Space Research* **74**(3). <https://doi.org/10.1016/j.asr.2024.05.003>.
16. Neves, MC et al. 2020. Evaluation of GRACE data for water resource management in Iberia: A case study of groundwater storage monitoring in the Algarve region. *J. Hydrol. Reg. Stud.* **32**. 100734. <https://doi.org/10.1016/j.ejrh.2020.100734>.
17. Pasik, A et al. 2023. Uncertainty estimation for a new exponential-filter-based long-term root-zone soil moisture dataset from Copernicus Climate Change Service (C3S) surface observations *Geosci. Model Dev.* **16**, p. 4957–4976, <https://doi.org/10.5194/gmd-16-4957-2023>.
18. Prudhomme, C et al. 2024. Global hydrological reanalyses: The value of river discharge information for world-wide downstream applications – The example of the Global Flood Awareness System GloFAS. *Meteorological Applications* **31**(2), <https://doi.org/10.1002/met.2192>.
19. Rakovec, O et al. 2022. The 2018–2020 Multi-Year Drought Sets a New Benchmark in Europe. *Earth's Future* **10**(3). <https://doi.org/10.1029/2021EF002394>.
20. Ramjeawon, M et al. 2022. Analyses of groundwater storage change using GRACE satellite data in the Usutu-Mhlathuze drainage region, north-eastern South Africa. *Journal of Hydrology: Regional Studies* **42**, 101118, <https://doi.org/10.1016/j.ejrh.2022.101118>.
21. Rzepecka, Z et al. 2016. Assessment of resultant groundwater calculated on the basis of GRACE and GLDAS models. 16th International Multidisciplinary Scientific Geoconference (SGEM 2016), Informatics, Geoinformatics And Remote Sensing Conference Proceedings, SGEM 2016, VOL II, pp.125-132
22. Rzepecka, Z et al. 2024. Groundwater Storage Variations across Climate Zones from Southern Poland to Arctic Sweden: Comparing GRACE-GLDAS Models with Well Data. *Remote Sensing* **16**(12). DOI 10.3390/rs16122104.
23. Silva, CGR et al. 2024. Multi-decadal groundwater observations reveal surprisingly stable levels in southwestern Europe. *Communication Earth Environmental Science* **5**(387). <https://doi.org/10.1038/s43247-024-01554-w>.
24. Thomas BF et al. 2017. GRACE groundwater drought index: evaluation of California Central Valley groundwater drought. *Remote Sensing Environ.* **198**:384-392, doi: 10.1016/j.rse.2017.06.026.
25. Xanke, J and Liesch, T 2022. Quantification and possible causes of declining groundwater resources in the Euro-Mediterranean region from 2003 to 2020. *Hydrogeology Journal* January. Springer. DOI: 10.1007/s10040-021-02448-

26. Zhang, R et al. 2020. Increased European heat waves in recent decades in response to shrinking Arctic sea ice and Eurasian snow cover. *NPJ Clim Atmos Sci* **3**(1):1–9. <https://doi.org/10.1038/s41612-020-0110-8>.
27. Zhang, Y et al. 2016. Improved Seasonal Mann–Kendall Tests for Trend Analysis in Water Resources Time Series. *Advances in Time Series Methods and Applications Fields Institute Communication* **78**. Springer, New York, NY. [https://doi.org/10.1007/978-1-4939-6568-7\\_10](https://doi.org/10.1007/978-1-4939-6568-7_10).
28. Zhao, K et al. 2023. Spatial-temporal variations of groundwater storage in China: A multiscale analysis based on GRACE data. *Resources, Conservation and Recycling* **197**, 107088, <https://doi.org/10.1016/j.resconrec.2023.107088>.

## APPENDIX 1:

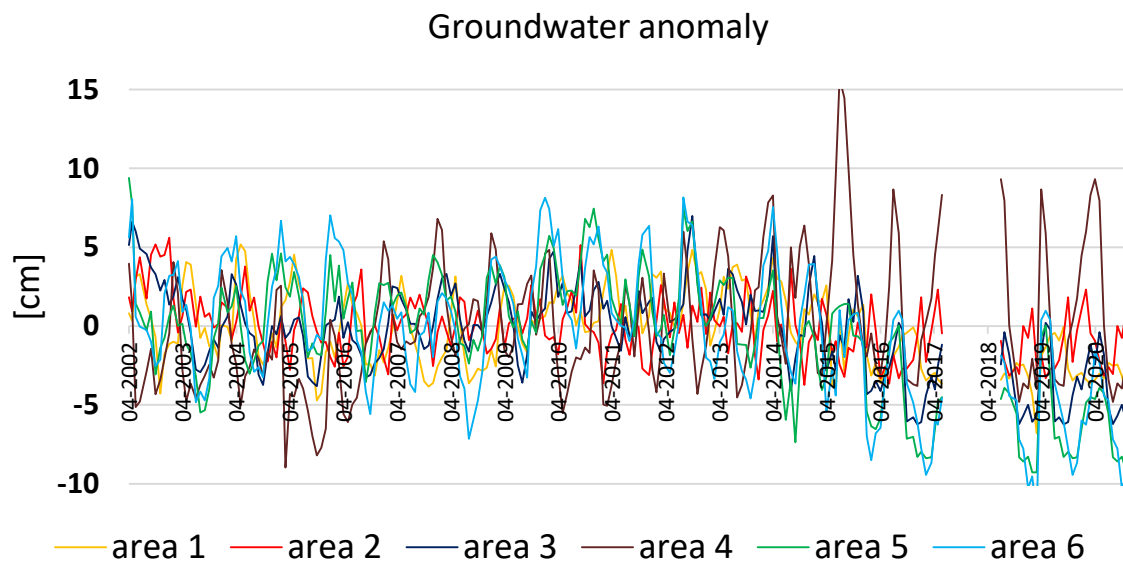


Fig.14. Groundwater anomaly for areas 1, 2, 3, 4, 5, 6.